

# 1 Stochastic and scaling climate sensitivities: Solar, volcanic 2 and orbital forcings

3 S. Lovejoy<sup>1</sup> and D. Schertzer<sup>2</sup>

4 Received 2 April 2012; accepted 30 April 2012; published XX Month 2012.

5 [1] Climate sensitivity ( $\lambda$ ) is usually defined as a deter-  
6 ministic quantity relating climate forcings and responses.  
7 While this may be appropriate for evaluating the outputs of  
8 (deterministic) GCM's it is problematic for estimating sen-  
9 sitivities from empirical data. We introduce a stochastic  
10 definition where it is only a statistical link between the  
11 forcing and response, an upper bound on the deterministic  
12 sensitivities. Over the range  $\approx 30$  yrs to 100 kyrs we estimate  
13 this  $\lambda$  using temperature data from instruments, reanalyses,  
14 multiproxies and paleo sources; the forcings include sev-  
15 eral solar, volcanic and orbital series. With the exception of  
16 the latter - we find that  $\lambda$  is roughly a scaling function of  
17 resolution  $\Delta t$ :  $\lambda \approx \Delta t^{H_\lambda}$ , with exponent  $0 \approx H_\lambda \approx 0.7$ .  
18 Since most have  $H_\lambda > 0$ , the implied feedbacks must gen-  
19 erally increase with scale and this may be difficult to achieve  
20 with existing GCM's. **Citation:** Lovejoy, S., and D. Schertzer  
21 (2012), Stochastic and scaling climate sensitivities: Solar, volcanic  
22 and orbital forcings, *Geophys. Res. Lett.*, 39, LXXXXX,  
23 doi:10.1029/2012GL051871.

## 24 1. Introduction

25 [2] Even if one accepts that orbital forcing is the “pae-  
26 ce-maker of the ice ages” [*Hays et al.*, 1976], over the range  
27  $\approx 30$  yrs to  $\approx 30$  kyrs, there is no doubt that most of the var-  
28 iance in paleotemperature records is associated with the  
29 continuous spectral “background” [*Lovejoy and Schertzer*,  
30 1986; *Wunsch*, 2003] (for a recent spectrum see Figure S1  
31 in Text S1 in the auxiliary material).<sup>1</sup> This strongly suggests  
32 that other internal and/or external mechanisms are needed to  
33 explain the multidecadal, multicentennial and multimillennial  
34 variability. The discussion of these issues has been strongly  
35 tinted by the development of GCM's and their response to  
36 various external climate forcings. However, if the amplifi-  
37 cation factors are large – as they must be – then it will be  
38 hard to distinguish nominally external forcing paradigms  
39 from purely internal ones.

40 [3] The usual approach to evaluating climate forcings is  
41 via the climate sensitivity ( $\lambda$ ) defined as the equilibrium  
42 change in a quantity, (here the temperature) per unit of  
43 radiative forcing. Sensitivities ( $\lambda$ ) are commonly estimated

with the help of (deterministic) numerical models; the usual  
example being the doubling of CO<sub>2</sub>. The change in condi-  
tions (compositional in this example) simultaneously leads  
to changes in the typical mean global temperature ( $\Delta T$ ) and  
to the earth's radiative equilibrium from which the radiative  
forcing ( $\Delta R_F$ ) is determined by:

$$\Delta T = \lambda \Delta R_F \quad (1)$$

This definition of climate sensitivity is convenient for  
numerical experiments with strong anthropogenic forcings.  
In this case, the response is relatively regular (smooth) so  
that the estimate  $\lambda = \Delta R_F(\Delta t) / \Delta T(\Delta t)$  is well defined,  
insensitive to  $\Delta t$ . However, for natural forcings, it has sev-  
eral shortcomings. First, GCM outputs fluctuate over a wide  
range of  $\Delta t$  so that – except for very small time scales  
comparable to the model integration time steps - fluctuations  
 $\Delta T(\Delta t)$  (and presumably)  $\Delta R_F(\Delta t)$  typically have non-  
trivial scaling behaviours  $\Delta T(\Delta t) \approx \Delta t^{H_T}$  and  $\Delta R_F(\Delta t) \approx$   
 $\Delta t^{H_R}$  implying  $\lambda(\Delta t) \approx \Delta t^{H_\lambda}$  with  $H_\lambda = H_T - H_R$  generally  
noninteger. Second, the usual definition of climate sensitiv-  
ity is only valid if there is a causal link: the fluctuations  $\Delta T$   
and  $\Delta R_F$  must have the same underlying cause such as a  
change in solar output. Strictly speaking, it therefore cannot  
be used empirically since in the real world there is only a  
single realization of climate. From the climate record, we  
can only measure correlations, not causality. In addition to  
the causality assumption, empirical estimates of  $\lambda$  must rely  
on model outputs in order to estimate  $\Delta R_F$  [e.g., *Harvey*,  
1988; *Claquin et al.*, 2003; *Chylek and Lohmann*, 2008;  
*Ganopolski and Schneider von Deimling*, 2008].

[4] As a consequence of these difficulties,  $\lambda$  has not been  
systematically explored as a function scale and it mostly  
known from models - not empirically. We therefore give a  
new stochastic definition of climate sensitivity which allows  
us to empirically estimate it for any physical forcing process  
whose consequent radiative forcing can be determined.

## 2. The Scaling of Temperatures, CO<sub>2</sub> Concentrations and Solar, Volcanic and Orbital Forcings

[5] Before considering potential climate drivers, let us first  
recall the variation with time scale  $\Delta t$  of temperature fluctu-  
ations  $\Delta T$ . For this purpose, it turns out that it is *not* suf-  
ficient to define the fluctuation as the absolute difference  $\Delta T$   
( $\Delta T = |T(t + \Delta t) - T(t)|$ ). Instead, we should use twice the  
absolute difference of the mean of the temperature between  $t$   
and  $t + \Delta t/2$  and between  $t + \Delta t/2$  and  $t + \Delta t$ . Technically, this  
corresponds to defining fluctuations using Haar wavelets  
rather than “poor man's” wavelets. While the latter is ade-  
quate for fluctuations increasing with scale (i.e.,  $\Delta T \approx \Delta t^{H_T}$   
with  $H_T > 0$ ), on average, absolute differences cannot

<sup>1</sup>Auxiliary materials are available in the HTML. doi:10.1029/2012GL051871.

<sup>2</sup>Physique Department, McGill University, Montreal, Quebec, Canada.  
<sup>3</sup>CERREVE, Ecole Nationale des Ponts et Chaussées, Marne-la-Vallée, France.

Corresponding author: S. Lovejoy, Physics Department, McGill University, 3600 University St., Montreal, QC H3A 2T8, Canada. (lovejoy@physics.mcgill.ca)

Copyright 2012 by the American Geophysical Union. 0094-8276/12/2012GL051871

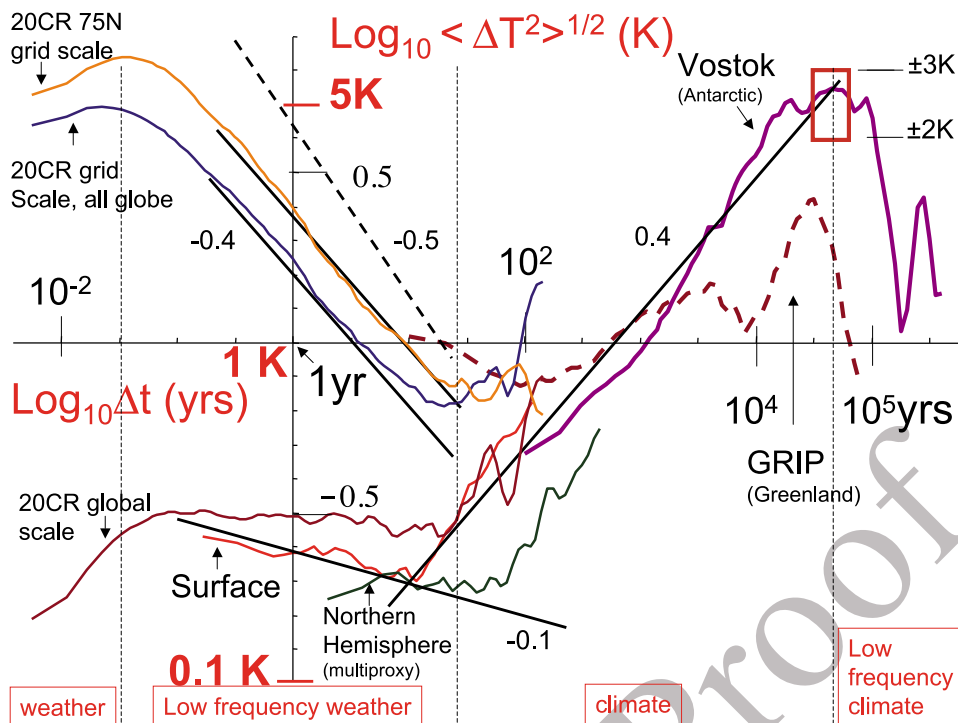


**Figure 1.** The RMS Haar structure function for temperatures including daily resolution 20th Century Reanalysis (20CR) data. On the left top we show grid point scale ( $2^\circ \times 2^\circ$ ) daily scale fluctuations for both  $75^\circ\text{N}$  and globally averaged along with reference slope  $\xi(2)/2 = -0.4 \approx H(20\text{CR}, 700 \text{ mb})$ . On the lower left, we see at daily resolution, the corresponding globally averaged structure function. Also shown are the average of three in situ surface series as well as a multiproxy structure function (northern hemisphere). At the right we show both the GRIP (55 cm resolution, with calibration constant 0.5 K/mil) and the Vostok paleotemperature series. Also shown is the interglacial “window”. See Lovejoy and Schertzer [2012b] for the figure and a full description of the data.

92 decrease and so when  $H_T < 0$ , do not correctly estimate  
 93 fluctuations. The Haar fluctuation (which is useful for  $-1 <$   
 94  $H_T < 1$ ) is particularly easy to understand since (with proper  
 95 “calibration”) in regions where  $H_T > 0$ , it can be made very  
 96 close to the difference fluctuation and in regions where  $H_T <$   
 97 0, it can be made close to another simple to interpret “ten-  
 98 dency fluctuation” (for discussion, see Lovejoy and  
 99 Schertzer [2012b]).

100 [6] The variation of the fluctuations with scale can be  
 101 defined using their statistics; the “generalized”  $q$ th order  
 102 structure function  $S_q(\Delta t)$  is particularly convenient:

$$S_q(\Delta t) = \langle \Delta T(\Delta t)^q \rangle \quad (2)$$

103 where “ $\langle \cdot \rangle$ ” indicates ensemble averaging. In a scaling  
 104 regime,  $S_q(\Delta t)$  is a power law;  $S_q(\Delta t) \approx \Delta t^{\xi(q)}$ , where the  
 105 exponent  $\xi(q) = qH - K(q)$  and  $K(q)$  characterizes the  
 106 scaling intermittency (satisfying  $K(1) = 0$ ). Below, with  
 107 the exception of the volcanic series (where  $K(2) \approx 0.2$ ),  $K(2)$   
 108 is small ( $\approx 0.01 - 0.03$ ), so that the RMS variation  $S_2(\Delta t)^{1/2}$   
 109 has the exponent  $\xi(2)/2 \approx \xi(1) = H$ . Note that when  $q = 2$  (the  
 110 classical structure function), we have the useful relation  $\xi(2)$   
 111  $= \beta - 1$  where  $\beta$  is the spectral exponent defined by the  
 112 spectral density  $E(\omega) \approx \omega^{-\beta}$  where  $\omega$  is the frequency.

113 [7] When  $S_2(\Delta t)^{1/2}$  is estimated for various in situ,  
 114 reanalysis, multiproxy and paleo temperatures, then one  
 115 obtains Figure 1 (see Table S1 in Text S1). The key points to  
 116 note are a) the three qualitatively different regimes: weather,  
 117 low frequency weather and climate with RMS fluctuations

118 respectively increasing, decreasing and increasing again  
 119 with scale ( $H_w > 0$ ,  $H_{lw} < 0$ ,  $H_c > 0$ ) and with transitions at  
 120  $\tau_w \approx 5-10$  days and  $\tau_c \approx 10-30$  yrs, b) the difference  
 121 between the local and global fluctuations, with the former  
 122 decreasing from  $\approx 5$  K (10 days) to  $\approx 0.6$  K at  $\approx 25$  yrs,  
 123 increasing to  $\approx 5$  K at 50 kyrs c) the “glacial/interglacial  
 124 window” corresponding to overall  $\pm 3$  to  $\pm 5$ K variations  
 125 over scales with half periods of 30 – 50 kyrs. This basic  
 126 multiscaling regime picture is similar to that of Lovejoy and  
 127 Schertzer [1984, 1986], Pelletier [1998], and Huybers and  
 128 Curry [2006]. For comparison, we could note that unforced  
 129 GCM’s (control runs) at grid scale resolution have  $H_{lw} \approx$   
 130  $-0.4$  and do not yield any climate regime; i.e.,  $\tau_c \rightarrow \infty$  [see  
 131 Lovejoy and Schertzer, 2012a].

132 [8] The problem of climate forcing is thus to determine  
 133 what forcings might end the (decreasing,  $H < 0$ ) low fre-  
 134 quency weather regime and cause the fluctuations to start to  
 135 increasing again when  $\Delta t > \tau_c$  (i.e.,  $H > 0$ )? To answer this,  
 136 let us consider various possible external drivers as functions  
 137 of scale; these may be conveniently classified according to  
 138 whether they are scaling or nonscaling. This is useful  
 139 because nonscaling climate forcings - i.e., at well defined  
 140 frequencies - would leave strong signatures in the form of  
 141 breaks in the temperature (and other) scalings which are  
 142 generally not observed over the range of time scales between  
 143  $\tau_c \approx 10 - 30$  yrs and  $\tau_{lc} \approx 50-100$  kyrs.

144 [9] An important nonscaling driver is the narrow-band  
 145 orbital forcings at scales somewhat shorter but close enough  
 146 to the upper time scale  $\tau_{lc}$ . Although this break may well be

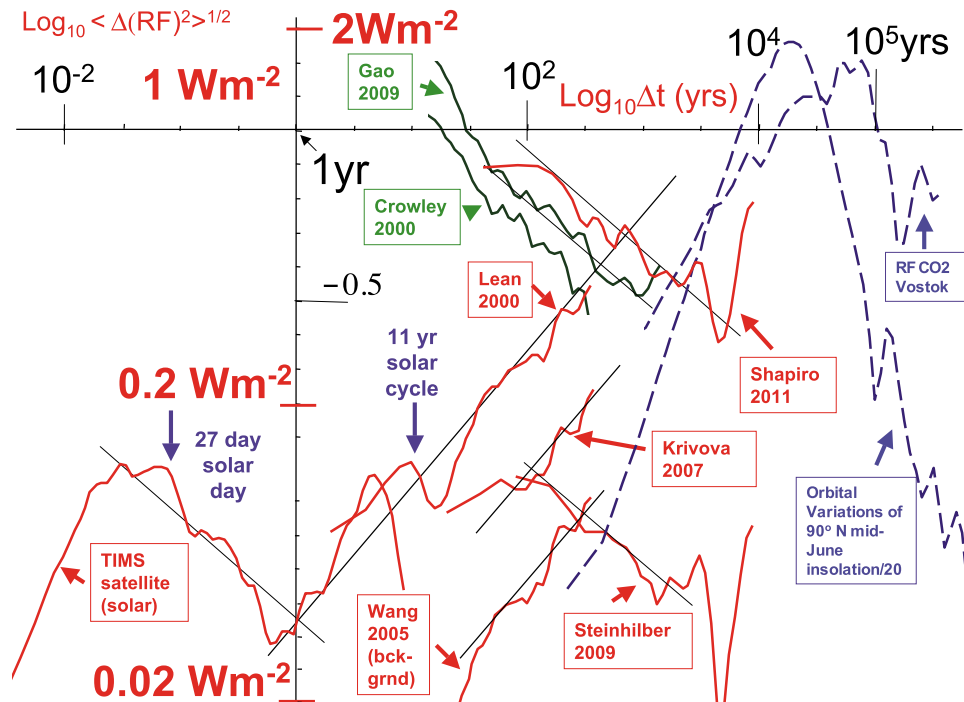


**Figure 2.** An intercomparison of RMS Haar fluctuations for various solar, volcanic, orbital and CO<sub>2</sub> data in units of radiative forcing ( $R_F$ ) the solar radiances, the values of estimated Total Solar Insolation were converted into  $R_F$  using an albedo = 0.7 and geometric factor 1/4. The Tims satellite data is for 8.7 yrs from 2003 to the present at a 6 hr resolution. Note that the Lean, 2000 reconstruction includes the 11 solar cycle whereas the Wang 2005 curve is only for the background. The Krivova 2007 curve has a 10 yr resolution. The Shapiro curve (the last 8963 yrs) was degraded to 20 yr resolution to average out the solar cycle, the Steinhilber curve was at a 40 yr and resolution over the last 9300 yrs. The volcanic series were from reconstructions of stratospheric sulphates using ice core proxies; due to the use of a 31 yr smoother, only results for longer scales are indicated in the figure (for reference the raw  $DR_F(Dt = 2 \text{ yrs}) \approx 5 \text{ Wm}^{-2}$ ). The Vostok paleo CO<sub>2</sub> series were converted to  $R_F$  using 3.7 W/m<sup>2</sup> per CO<sub>2</sub> doubling, the solar insolation at the north pole on June 15th was divided by 20, it is not a true  $R_F$ . The orbital variation curve was interpolated to 100 yr resolution and the low and high frequency fall-offs have logarithmic slopes  $-1, 1$ , i.e., they are the minimum and maximum possible for these Haar fluctuations. All the structure functions have been increased by a factor of 2 so that they are roughly “calibrated” with the difference ( $H > 0$ ) and tendency ( $H < 0$ ) fluctuations.

147 compatible with the observations, this is not trivial since the  
 148 main signal in the temperature is nearer 100 kyr  
 149 corresponding to orbital eccentricity variations. At least at  
 150 high latitudes, these are much weaker not only than the  
 151 higher frequency precessional and obliquity variations, but  
 152 also than the lower frequency 400 kyrs eccentricity varia-  
 153 tions whose signal is virtually absent in the paleoclimate  
 154 record; the “100 kyr” and “400 kyr” problems [Ganopolski  
 155 and Calov, 2011; see also Berger et al., 2005]. To quantify  
 156 the orbital forcing, Figure 2 shows  $S_2(\Delta t)^{1/2}$  of the solar  
 157 irradiance variations at the north pole (every June 15th)  
 158 determined from astronomical calculations [Berger and  
 159 Loutre, 1991]. While this is not a true radiative forcing, it  
 160 indicates its dominant time scales. One sees that the vari-  
 161 ability is confined to a fairly narrow range of scales and in  
 162 Figure 3 we see that this range is about 3–4 times smaller  
 163 than that of the peak in the paleotemperature variability; this  
 164 is the 100 kyrs problem.

165 [10] Turning to the higher frequency continuous back-  
 166 ground, an (apparently) attractive possibility is to invoke  
 167 greenhouse gas forcings. For example, using the recommended  
 168 value 3.7 W/m<sup>2</sup> for a CO<sub>2</sub> doubling [Intergovernmental Panel  
 169 on Climate Change, 2007], Vostok paleo CO<sub>2</sub> concentrations

can be converted into radiative forcings (Figure 2). While to  
 within a constant factor (Figure 3) this is very nearly the same  
 as the corresponding temperature structure function, cross  
 spectral temperature - CO<sub>2</sub> analysis (Figure S2 in Text S1)  
 shows that over the whole range up to  $\omega \approx (6 \text{ kyr})^{-1}$ , that the  
 phase of the CO<sub>2</sub> fluctuations lags those of the temperature  
 by  $\approx 74 \pm 22^\circ$  so that (contrary to contemporary anthropo-  
 genic CO<sub>2</sub>) – the paleo CO<sub>2</sub> is a “follower” not a “driver”  
 (although it may play a role in solving the 100, 400 kyr  
 “problems” [Ganopolski and Calov, 2011]), it is shown in  
 Figures 2 and 3 for reference only.

[11] Quantifying solar variability is extremely difficult.  
 Since 1980, a series of satellites have estimated the Total  
 Solar Irradiance, yet the relative calibrations are not known  
 with sufficient accuracy to establish the decadal and longer  
 scale variability. Figure 2 shows  $S_2(\Delta t)^{1/2}$  from the 8 year  
 long series from the Tims satellite; we see clearly the 27  
 (earth) day long solar “day” followed by a low frequency  
 rise. To go further requires proxy based “reconstructions”,  
 Figure 2 shows  $S_2(\Delta t)^{1/2}$  from several of these using sun-  
 spots and <sup>10</sup>Be records. The earliest [Lean, 2000] used a two  
 component model, one of which had an 11 year cycle based  
 on the recorded sunspots back to 1610, the other was a

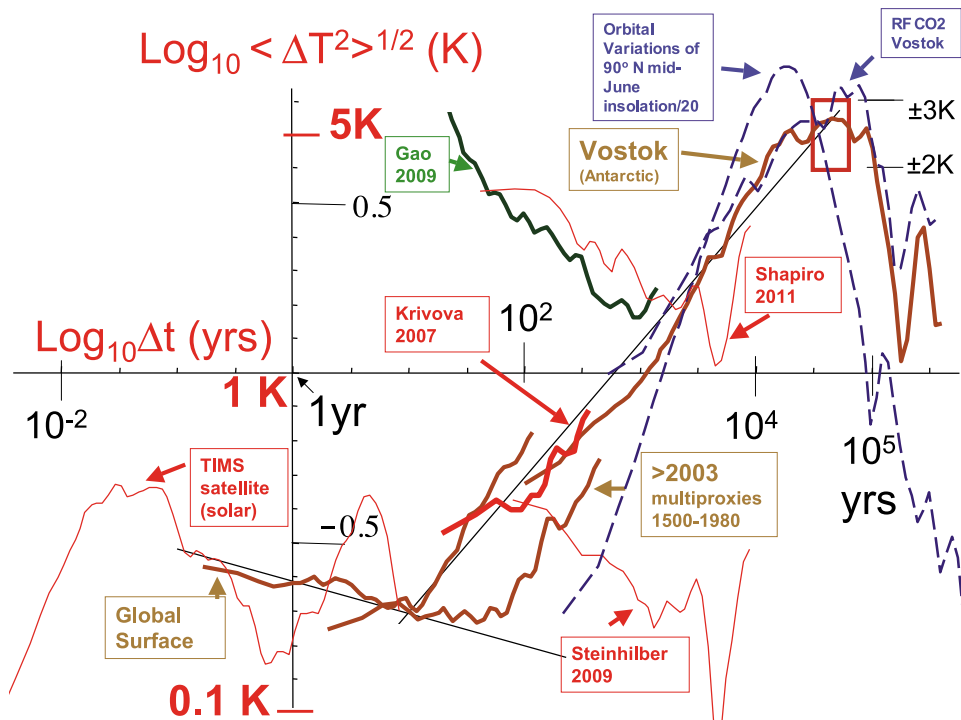


**Figure 3.** The RMS structure functions of the selected forcings from Figure 2 were converted into RMS temperature structure functions using a unique (and scale independent) climate sensitivity  $\lambda = 4.5 \text{ K}/(\text{Wm}^{-2})$ . The reference lines have slopes of  $-0.1$  and  $+0.4$ . It can be seen that the main orbital insolation fluctuations occur at time scales roughly 3–4 times smaller than the main temperature fluctuations.

193 “background”. Combining the two results leads to an annual  
 194 series featuring an overall 0.21% variation in the background  
 195 since the 17th century “Maunder Minimum”. Figure 2 shows  
 196 that this reconstruction actually meshes quite nicely with the  
 197 TAMS data with exponent  $\xi(2)/2 \approx H_{RF} \approx 0.4$ , i.e., close to  
 198  $H_T$  (Figure 3). Wang *et al.* [2005] updated this series and  
 199 found typical fluctuations  $\approx 4$ –5 times lower (Figure 2). A  
 200 little later an intermediate (but still sunspot based) estimate  
 201 yielded a variation of 0.1% since the Maunder minimum,  
 202 again with  $\xi(2)/2 \approx 0.4$  [Krivova *et al.*, 2007].

203 [12] The situation changed dramatically with the  $\approx 9$  kyr  
 204 long reconstructions of Steinhilber *et al.* [2009] and Shapiro  
 205 *et al.* [2011]. Both used ice core  $^{10}\text{Be}$  concentrations to  
 206 estimate the flux of cosmic rays, itself a proxy for the solar  
 207 magnetic field and hence of solar activity. Although both  
 208 were calibrated using the satellite observations, their  
 209 assumptions were quite different, notably about a hypothet-  
 210 ical “quiescent” solar state. The  $S_2(\Delta t)^{1/2}$  for these recon-  
 211 structions are remarkable for two reasons. First, they differ  
 212 from each other by a large factor ( $\approx 8$ –9, see Figure 2);  
 213 second, their slopes are the opposite to the sunspot based  
 214 estimates: rather than  $\xi(2)/2 \approx H \approx 0.4$ , they have  $\xi(2)/2 \approx$   
 215  $H \approx -0.3!$  While the large factor between them attracted  
 216 attention, the change in the sign of  $H$  was not noticed even  
 217 though it is probably more important as it would imply  
 218 amplification mechanisms that increase quite strongly with  
 219 scale.

220 [13] Another important driver is explosive volcanism.  
 221 Volcanoes mainly influence the climate through the emis-  
 222 sion of sulphates that reflect incoming solar radiation;  
 223 stratospheric sulphates can persist for months or years after  
 224 an eruption. The two main volcanic reconstructions

[Crowley, 2000; Gao *et al.*, 2008] are based on ice core  
 225 particulate concentrations. First, sulphate concentrations are  
 226 estimated and then with the help of models the  
 227 corresponding global radiative forcings are determined; for  
 228  $S_2(\Delta t)^{1/2}$ , see Figure 2. It is remarkably similar to that of the  
 229  $^{10}\text{Be}$  solar variabilities with  $\xi(2)/2 \approx -0.3$ , it nearly coin-  
 230 cides with  $S_2(\Delta t)^{1/2}$  from the Shapiro *et al.* [2011] solar  
 231 reconstruction. The slightly longer (1500 yrs) Gao *et al.*  
 232 [2008] series was converted into equivalent radiative forc-  
 233 ings by scaling the mean to the Crowley [2000] series, the  
 234  $S_2(\Delta t)^{1/2}$  results for the two series are very similar  
 235 (Figure 2). Although very strong at small  $\Delta t$ , the volcanic  
 236 forcings decrease rapidly at longer intervals so that any  
 237 mechanism responsible for temperature fluctuations must on  
 238 the contrary involve an amplification that strongly increases  
 239 with scale.  
 240

### 3. Stochastic and Scaling Climate Sensitivities 241

[14] We would like to be able to compare the  $T$  and  $R_F$   
 242 fluctuations (Figures 1 and 2) but strictly speaking, the  
 243 deterministic definition (equation (1)) doesn’t allow it. To  
 244 interpret our forcing and temperature statistics it is therefore  
 245 convenient to introduce a stochastic definition of climate  
 246 sensitivity:

$$\Delta T \stackrel{d}{=} \lambda \Delta R_F \quad (3)$$

where, “ $\stackrel{d}{=}$ ” means equality in the sense of random variables  
 247 the random variables  $a, b$  satisfy  $a \stackrel{d}{=} b$  if and only if  $\Pr$   
 248  $(s) = \Pr(b > s)$  for all  $s$ , “Pr” means “probability”. Notice  
 249 that while both deterministic and stochastic definitions  
 250



251 (equations (1) and (3)) predict that the statistical moments  
 252 are related by the equation  $\langle \Delta T^q \rangle = \lambda^q \langle (\Delta R_F)^q \rangle$ , the sto-  
 253 chastic definition doesn't even require that  $R_F$  and  $T$  be  
 254 correlated. A convenient interpretation is to regard the sto-  
 255 chastic  $\lambda$  (equation (3)) as an upper bound on the deter-  
 256 ministic  $\lambda$  with equality in case of full (and causal)  
 257 correlation. The advantage of adopting equation (3) is that  
 258 by fixing  $\lambda$ , we may convert Figure 2 into equivalent tem-  
 259 perature fluctuations; Figure 3 shows the resulting super-  
 260 positions using  $\lambda = 4.5 \text{ K}/(\text{Wm}^{-2})$  throughout. To put this  
 261 value in perspective, we can compare it to  $\lambda_0 \approx 0.3 \text{ K}/$   
 262  $(\text{Wm}^{-2})$ , the sensitivity of the simplest energy balance  
 263 model involving a homogenous atmosphere and radiative  
 264 equilibria. We see that a (large) "feedback" factor  $f = \lambda/\lambda_0 =$   
 265  $4.5/0.3 \approx 15$  is necessary to justify the overlaps shown in the  
 266 figure.

267 [15] From equation (3) - and for simplicity only consider-  
 268 ing the mean ( $q = 1$ ) behaviour - we see that if  $\langle \Delta T(\Delta t) \rangle \propto$   
 269  $\Delta t^{H_T}$  and  $\langle \Delta R_F(\Delta t) \rangle \propto \Delta t^{H_{RF}}$ , then  $H_\lambda = H_T - H_{RF}$ . If we  
 270 take  $H_{RF} \approx -0.3$  (volcanic and  $^{10}\text{Be}$  solar estimates),  $H_{RF}$   
 271  $\approx 0.4$  (sunspot based solar) and  $H_T \approx 0.4$ , then we find  $H_\lambda \approx$   
 272  $0.7$  and  $\approx 0$  respectively. From Figure 2 we see that the vol-  
 273 canic and Shapiro *et al.* [2011] solar forcings require a  
 274 feedback factor  $f \approx 0.3$  at 30 year scales, rising to roughly  
 275  $\approx 20$  at 10 kyrs. If we consider instead the scale independent  
 276 amplification factors ( $H_\lambda \approx 0$ ), i.e., the Krivova and Wang  
 277 reconstructions, we find the (scale independent) factors  
 278  $f \approx 15, 30$  respectively. However, for this to apply at mul-  
 279 timillennial scales, solar variability must continue to grow  
 280 reaching  $\approx 1 \text{ Wm}^{-2}$  at 10 kyr scales.

#### 281 4. Conclusions

282 [16] After decreasing over several decades of scale, to a  
 283 minimum of  $\approx \pm 0.1 \text{ K}$  at around 10–100 yrs, temperature  
 284 fluctuations begin to increase, ultimately reaching  $\pm 3$  to  
 285  $\pm 5 \text{ K}$  at glacial-interglacial scales. In order to understand the  
 286 origin of this multidecadal, multicentennial and multi-  
 287 millennial variability, we empirically estimated the climate  
 288 sensitivities of solar and volcanic forcings using several  
 289 reconstructions. To make this practical, we introduced a  
 290 stochastic definition of the sensitivity which could be  
 291 regarded as an upper bound on the usual (deterministic)  
 292 sensitivity with the two being equal in the case of full (and  
 293 causal) correlation between the temperature and driver.  
 294 Although the RMS temperature fluctuations increased with  
 295 scale, the RMS volcanic and  $^{10}\text{Be}$  based solar reconstruc-  
 296 tions all decreased with scale, in roughly a power law  
 297 manner. If any of these reconstructions represented domi-  
 298 nant forcings, the corresponding feedbacks would have to  
 299 increase strongly with scale (with exponent  $H_\lambda \approx 0.7$ ), and  
 300 this is not trivially compatible with existing GCM's. Only  
 301 the sunspot based solar reconstructions were consistent with  
 302 scale independent sensitivities ( $H_\lambda \approx 0$ ), these are of the  
 303 order  $4.5 \text{ K}/(\text{Wm}^{-2})$  (i.e., implying large feedbacks) and  
 304 would require quite strong solar forcings of  $\approx 1 \text{ Wm}^{-2}$  at  
 305 scales of 10 kyrs.

306 [17] A recent analysis of  $S_2(\Delta t)^{1/2}$  for forced GCM out-  
 307 puts over the past millennium S. Lovejoy *et al.* (Do GCM's  
 308 predict the climate.... Or low frequency weather?, submitted  
 309 to *Nature Climate Change*, 2012) showed that they strongly  
 310 underestimate the low frequency variability – even when for

example strong solar forcings were used. Our findings here 311  
 of the occasionally surprising scale-by-scale forcing vari- 312  
 abilities helps explain why they were too weak. It seems 313  
 likely that GCM's are a missing an important mechanism of 314  
 internal variability. A possible candidate is land-ice whose 315  
 fluctuations are plausibly scaling over the appropriate ranges 316  
 of space-time scale, but which is not yet integrated into 317  
 existing GCM's. 318

#### References

- Berger, A., and M. F. Loutre (1991), Insolation values for the climate of the 320  
 last 10 million years, *Quat. Sci. Rev.*, 10, 297–317, doi:10.1016/0277- 321  
 3791(91)90033-Q. 322
- Berger, A., J. L. Mélice, and M. F. Loutre (2005), On the origin of the 323  
 100-kyr cycles in the astronomical forcing, *Paleoceanography*, 20, 324  
 PA4019, doi:10.1029/2005PA001173. 325
- Chylek, P., and U. Lohmann (2008), Aerosol radiative forcing and climate 326  
 sensitivity deduced from the last glacial maximum to Holocene transi- 327  
 tion, *Geophys. Res. Lett.*, 35, L04804, doi:10.1029/2007GL032759. 328
- Claquin, T., et al. (2003), Radiative forcing of climate by ice-age atmo- 329  
 spheric dust, *Clim. Dyn.*, 20, 193–202. 330
- Crowley, T. J. (2000), Causes of climate change over the past 1000 years, 331  
*Science*, 289, 270–277, doi:10.1126/science.289.5477.270. 332
- Ganopolski, A., and R. Calov (2011), The role of orbital forcing, carbon 333  
 dioxide and regolith in 100 kyr glacial cycles, *Clim. Past*, 7, 334  
 1415–1425, doi:10.5194/cp-7-1415-2011. 335
- Ganopolski, A., and T. Schneider von Deimling (2008), Comment on "Aero- 336  
 sol radiative forcing and climate sensitivity deduced from the Last Glacial 337  
 Maximum to Holocene transition" by Petr Chylek and Ulrike Lohmann, 338  
*Geophys. Res. Lett.*, 35, L23703, doi:10.1029/2008GL033888. 339
- Gao, C., A. Robock, and C. Ammann (2008), Volcanic forcing of climate 340  
 over the past 1500 years: An improved ice core-based index for climate 341  
 models, *J. Geophys. Res.*, 113, D23111, doi:10.1029/2008JD010239. 342
- Harvey, D. (1988), Climatic impact of ice-age aerosols, *Nature*, 334, 343  
 333–335, doi:10.1038/334333a0. 344
- Hays, J. D., et al. (1976), Variations in the Earth's orbit: Pacemaker of the 345  
 Ice Ages, *Science*, 194, 1121–1132, doi:10.1126/science.194.4270.1121. 346
- Huybers, P., and W. Curry (2006), Links between annual, Milankovitch and 347  
 continuum temperature variability, *Nature*, 441, 329–332, doi:10.1038/ 348  
 nature04745. 349
- Intergovernmental Panel on Climate Change (2007), *Climate Change 2007: 350  
 The Physical Science Basis. Contribution of Working Group I to the 351  
 Fourth Assessment Report of the Intergovernmental Panel on Climate 352  
 Change*, edited by S. Solomon et al., Cambridge Univ. Press, Cambridge, 353  
 U. K. 354
- Krivova, N. A., et al. (2007), Reconstruction of solar total irradiance 355  
 since 1700 from the surface magnetic field flux, *Astron. Astrophys.*, 356  
 467, 335–346, doi:10.1051/0004-6361:20066725. 357
- Lean, J. L. (2000), Evolution of the Sun's spectral irradiance since the 358  
 Maunder Minimum, *Geophys. Res. Lett.*, 27, 2425–2428, doi:10.1029/ 359  
 2000GL000043. 360
- Lovejoy, S., and D. Schertzer (1984), 40 000 years of scaling in climatolog- 361  
 ical temperatures, *Meteorol. Sci. Tech.*, 1, 51–54. 362
- Lovejoy, S., and D. Schertzer (1986), Scale invariance in climatological 363  
 temperatures and the spectral plateau, *Ann. Geophys.*, 4B, 401–410. 364
- Lovejoy, S., and D. Schertzer (2012a), *The Weather and Climate: Emergent 365  
 Laws and Multifractal Cascades*, 660 pp., Cambridge Univ. Press, 366  
 Cambridge, U. K. 367
- Lovejoy, S., and D. Schertzer (2012b), Low frequency weather and the 368  
 emergence of the climate, paper presented at Chapman Conference on 369  
 Complexity and Extreme Events in Geosciences, AGU, Hyderabad, 370  
 India, 15–19 Feb. 371
- Pelletier, J. D. (1998), The power spectral density of atmospheric tempera- 372  
 ture from scales of  $10^{-2}$  to  $10^6$  yr, *Earth Planet. Sci. Lett.*, 158, 157–164, 373  
 doi:10.1016/S0012-821X(98)00051-X. 374
- Shapiro, A. I., et al. (2011), A new approach to long-term reconstruction of 375  
 the solar irradiance leads to large historical solar forcing, *Astron. Astro- 376  
 phys.*, 529, A67, doi:10.1051/0004-6361/201016173. 377
- Steinhilber, F., J. Beer, and C. Fröhlich (2009), Total solar irradiance 378  
 during the Holocene, *Geophys. Res. Lett.*, 36, L19704, doi:10.1029/ 379  
 2009GL040142. 380
- Wang, Y.-M., et al. (2005), Modeling the Sun's magnetic field and irradi- 381  
 ance since 1713, *Astrophys. J.*, 625, 522–538, doi:10.1086/429689. 382
- Wunsch, C. (2003), The spectral energy description of climate change 383  
 including the 100 ky energy, *Clim. Dyn.*, 20, 353–363. 384